

ISCI, Volume 12

Supplemental Information

TRAIL-Expressing Monocyte/Macrophages

Are Critical for Reducing

Inflammation and Atherosclerosis

Siân P. Cartland, Scott W. Genner, Gonzalo J. Martínez, Stacy Robertson, Maaïke Kockx, Ruby CY. Lin, John F. O'Sullivan, Yen Chin Koay, Pradeep Manuneehi Cholan, Melkam A. Kebede, Andrew J. Murphy, Seth Masters, Martin R. Bennett, Wendy Jessup, Leonard Kritharides, Carolyn Geczy, Sanjay Patel, and Mary M. Kavoura

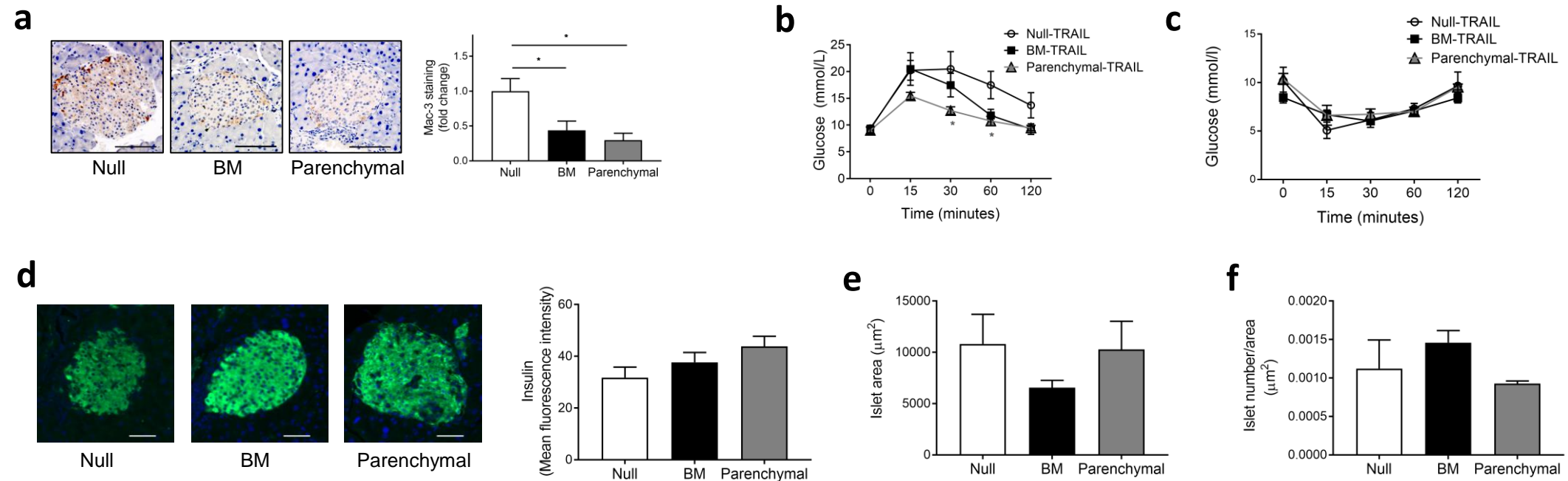


Figure S1. Parenchymal-TRAIL reduces improves glucose clearance and islet function. (a) Mac3+ immunoreactivity in pancreatic islets of BMT mice. Left panel is representative samples from null-, BM- and parenchymal TRAIL mice. Right panel represents quantification of staining. (b) glucose and (c) insulin tolerance testing in BMT mice. (d) Insulin immunoreactivity in islets of BMT mice is unaltered, left. Right panel represents quantification of staining. (e) Islet area and (f) number of islets/area is unchanged in BMT mice. Scale bar, 50 μm . Results are Mean \pm SEM. One-way ANOVA (n=5-8/group); * p <0.05.

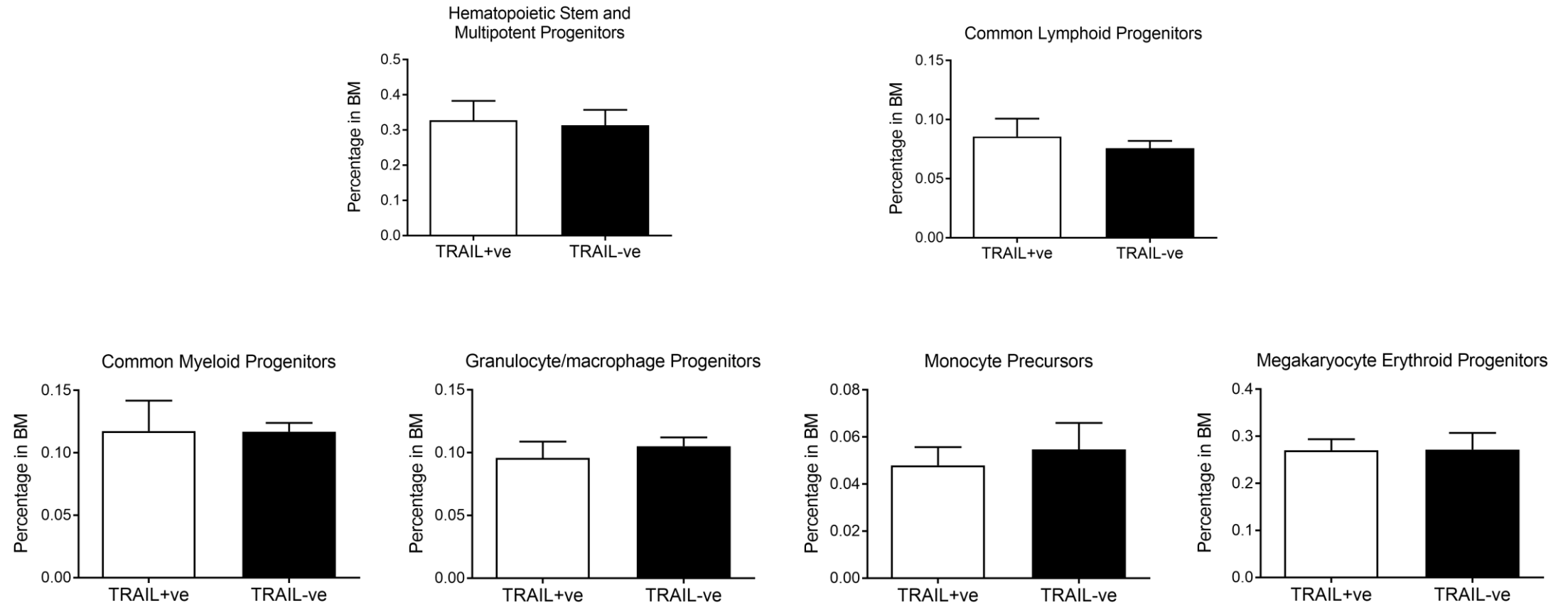


Figure S2. TRAIL deletion does not affect hematopoietic stem cell numbers. Percentage of progenitor cells in bone marrow of 6 w *Trail*^{-/-}*Apoe*^{-/-} (TRAIL-ve) and *Apoe*^{-/-} (TRAIL+ve) mice is not significantly different (n=5/genotype). Results are Mean ± SEM.

SUPPLEMENTARY TABLES

Table S1. Details of control, stable and unstable CAD patients. Related to Figures 1 and 6.
(Martinez et al., 2015)

Patient Characteristics	Control n=8	Stable CAD n=15	Unstable CAD n=12
Age (y) Mean (SD)	59.3 (5.7)	63.1 (9.3)	64.4 (11.6)
Female (%)	1 (13)	1 (7)	0 (0)
Diabetes mellitus (%)	1 (14)	4 (27)	3 (25)
Hypertension (%)	2 (29)	7 (47)	8 (67)
Dyslipidaemia (%)	3 (43)	9 (60)	10 (83)
Family history (%)	0 (0)	4 (27)	2 (17)
Current smoker (%)	3 (43)	4 (27)	3 (25)
Previous MI (%)	1 (13)	4 (27)	2 (17)
Previous PCI (%)	1 (13)	6 (40)	1 (8)
Previous CABG (%)	0 (0)	3 (20)	1 (8)
Renal impairment (%)	0 (0)	2 (13)	2 (17)

PCI, percutaneous coronary intervention; MI, myocardial infarction; CABG, coronary artery bypass graft.

Table S2. Details of CAD patients (2nd cohort). Related to Figure 1. (Robertson et al., 2016)

Patient Characteristics	(n=11)
Age (y) Mean (SD)	67.55 (14.57)
Female (%)	3 (27)
Diabetes mellitus (%)	4 (36)
Hypertension (%)	10 (91)
Dyslipidaemia (%)	8 (73)
Family history (%)	5 (46)
Current smoker (%)	3 (27)
Previous MI (%)	6 (55)
Previous PCI (%)	3 (27)
Previous CABG (%)	3 (27)
Renal impairment (%)	3 (27)

PCI, percutaneous coronary intervention; MI, myocardial infarction; CABG, coronary artery bypass graft.

Table S3. Primer sequences. Related to Figures 1-6.

Human 5'-3'		
	Forward	Reverse
TRAIL	ACCAACGAGCTGAAGCAGAT	CAAGTGCAAGTTGCTCAGGA
TNF-α	GTTGTAGCAAACCCTCAAGCTG	GAGGTACAGGCCCTCTGATG
NFκB p65	GGTCCACGGCGGACCGGT	GACCCCGAGAACGTGGTGC GC
Sp1	CCATACCCCTTAACCCCG	GAATTTTCACTAATGTTTCCCACC
GAPDH	GAAGGCTGGGGCTCATT	CAGGAGGCATTGCTGATGAT
Murine 5'-3'		
	Forward	Reverse
ABCA1	AAAACCGCAGACATCCTTCAG	CATACCGAAACTCGTTCACCC
ABCG1	CGAGAGGGCATGTGTGACG	CCGAGAAGCTATGGCAACC
CCL2	GCTGGAGCATCCACGTGTT	ATCTTGCTGGTGAATGAGTAGCA
CD11b	ATGGACGCTGATGGAATACC	TCCCCATTCACGTCTCCCA
CD36	AGATGACGTGGCAAAGAACAG	CCTTGGCTAGATAACGA ACTCTG
F4/80	CTTTGGCTATGGGCTTCCAGTC	GCAAGGAGGACAGAGTTTATCGTG
IL-10	GCTGGACAACATACTGCTAACC	ATTTCCGATAAAGGCTTGGCAA
IL-18	GACTCTTGCGTCAACTTCAAGG	CAGGCTGTCTTTTGTCAACGA
IL-1β	GTTTCTGCTTTCACCACTCCA	GAGTCCAATTTACTCCAGGTCAG
IL-6	CTGCAAGAGACTTCCATCCAG	AGTGGTATAGACAGGTCTGTTGG
iNOS	CGAAACGCTTCACTTCCAA	TGAGCCTATATTGCTGTGGCT
MerTK	CTCCTGAGCCCGTCAATATCT	AGACCAGGTACGGTTAGGACA
SRA	GGCAATGACTTTGGTACACAGT	TGGTGGTAGTCTTCGGCATAG
SRB1	TTTGGAGTGGTAGTAAAAAGGGC	TGACATCAGGGACTCAGAGTAG
TNF-α	CATCTTCTCAA AATTCGAGTGACAA	TGGGAGTAGACAAGGTACAACCC
TRAIL	CAGGCTGTGTCTGTGGCTGT	TGAGAAGCAAGCTAGTCCAATTTTG
β-Actin	AACCGTGAAAAGATGACCCAGAT	CACAGCCTGGATGGCTACGTA

TRANSPARENT METHODS

Patient studies- Patients presenting for cardiac catheterization at The Royal Prince Alfred Hospital, Sydney Australia, and previously recruited by us were used: (i) control (ii) stable and (iii) unstable CAD (Table S1). The control group were deemed to have no significant coronary disease as identified during angiography (Martinez et al., 2015). Blood was drawn from the aortic root, right atrium and coronary sinus prior to the procedure (Martinez et al., 2015). A second cohort of patients presenting with unstable CAD (n=11) had peripheral venous blood drawn within 24 h of admission. Venous blood from 7 healthy individuals served as controls. Patient details as previously reported are listed in Table S2 (Robertson et al., 2016). All procedures were conducted in accordance with the Sydney Local Health District Human Ethics Committee (X12-0241; Sydney, Australia) and all patients gave written informed consent before participating.

Human ELISAs –TRAIL and TNF- α in blood plasma were quantified according to the manufacturer's instructions (R&D Systems Inc.).

Human monocyte isolation – Peripheral blood mononuclear cells (PBMC) isolated as described (Robertson et al., 2016), were suspended in DMEM (Gibco) supplemented with 5% fetal bovine serum (FBS). PBMC (8×10^4 /well) were seeded onto 48-well plates (Corning) and non-adherent leukocytes removed 1 h later. Buffy coats (Australian Red Cross Blood Service) were used for IL-18 treatments. Isolated white cells were separated, and fractions examined using Wrights' stain (DiffQuik; Laboratory-Aids) (Ravindran et al., 2017). Monocytes were resuspended in serum-free RPMI 1640 (Gibco) containing penicillin (10 μ g/ml), streptomycin (10 μ g/ml), and L-glutamine (2 mM), and within 3 h of plating, cells were exposed to 10% human serum and recombinant IL-18 (30 ng/ml; R&D Systems) for 24 h at 37° C in a humidified atmosphere of 5% CO₂. All procedures were conducted in accordance with the Sydney Local Health District Human Ethics Committee (Reference X9.5/JUL17; Sydney, Australia).

Animal studies – *Trail*^{-/-}*Apoe*^{-/-}, *Apoe*^{-/-} and *Trail*^{-/-} and wildtype littermate control mice are described by us (Cartland et al., 2017; Di Bartolo et al., 2011), bred at Australian BioResources (NSW, Australia)

and backcrossed 6 generations since 2013 and 2014, and at least 10 generations prior to 2007 (Cartland et al., 2017; Di Bartolo et al., 2011). C57Bl6/J (wildtype; IMSR_JAX:000664) mice were purchased from Australian Resources Centre (WA, Australia) or Australian BioResources. For studies involving a “Western” high fat diet (HFD; Specialty feeds; WA, Australia), 6 w old mice were placed on the diet for up to 12 w (Di Bartolo et al., 2011). After an overnight fast, mice were anaesthetized by i.p. injection of ketamine (100 mg/kg) and xylazine (10 mg/kg), or by inhalation of 2% isoflurane prior to euthanasia by cardiac exsanguination. Plasma isolated from blood was snap-frozen and stored at -80°C. Indicated tissues were collected for gene expression or immunohistochemistry (IHC). Protocols were approved by the Animal Care and Ethics Committee at University of New South Wales (08/105A; 11/54B) or the Sydney Local Health District Animal Ethics Committee (2014-014; 2013-049) (Sydney, Australia).

Bone marrow chimeras – 8 w old male *Trail*^{-/-}*Apoe*^{-/-} and *Apoe*^{-/-} mice were given a lethal dose of radiation (8-9 Gys), randomized, transplanted with 10⁷ bone marrow cells from *Trail*^{-/-}*Apoe*^{-/-} or *Apoe*^{-/-} mice 24 h later (Figure 2a), and given 4 w for chimerization as described by us (Stoneman et al., 2007; Yu et al., 2011; Zhao et al., 2010). Mice were then fed a HFD for 12 w and euthanized as above.

Macrophage depletion - 6 w old male *Trail*^{-/-}*Apoe*^{-/-} mice were placed on a HFD for 12 w. After 1 w, mice were randomized, given weekly i.p. injections of liposomes containing clodronate (15 mg/kg), or control PBS (both from Clodronateliposomes.com), then euthanized as above.

Glucose and insulin tolerance tests (GTT, ITT) - were performed 10 and 11 w into the HFD (Cartland et al., 2014).

Murine plasma chemistries - Plasma glucose was measured using a glucometer (Accu-check Performa, Roche). Insulin (Mercodia), cholesterol, triglycerides (all from Wako Diagnostics) and TRAIL (USCN Life Science Inc.) were assessed according to the manufacturer’s instructions.

Histology – Brachiocephalic artery (3 µm) and pancreata sections (5 µm) were stained with H&E to assess plaque or islet size. IHC was performed using anti-Mac3 (1:100, BD Biosciences) for macrophage infiltration and anti-caspase 3 to measure apoptosis (1:200, R&D Systems) (Di Bartolo et al., 2011). Immunofluorescence was performed on sections of pancreata using guinea pig anti-insulin (1:1000, Dako), and detected with anti-guinea pig Alexa 488 (1:500, ThermoFisher). All control

sections with primary antibody omitted were negative. Images were captured using an Olympus BX53, Zeiss Axio Imager Z2 or Zeiss Axio Scan.Z1 microscope. Plaque and islet size were measured using ImageJ and percent of positive staining/tissue image area quantified using Image-Pro Premier (Cybernetics); 20-30 islets/mouse were assessed (Di Bartolo et al., 2011).

Total RNA isolation, cDNA and quantitative PCR (qPCR) – RNA was isolated from human monocytes and bone marrow-derived macrophages using the RNeasy Isolation Kit (QIAGEN) or TRI Reagent (Sigma), and from homogenized aortic tissue, using the RNeasy Fibrous Tissue Mini Kit (QIAGEN) (Cartland et al., 2017; Robertson et al., 2016). RNA was reverse transcribed using the iScript cDNA synthesis kit (BioRad, Australia). Real-time PCR was performed using iQ SYBR in a CFX384 thermocycler (BioRad, Australia). Relative changes in mRNA expression were determined using the $2^{-\Delta\Delta C_T}$ method normalized to housekeeping genes GAPDH or β -actin. Human and murine primer sequences are in Table S3.

Mouse macrophages – Bone marrow flushed from femurs and tibiae of *Trail^{-/-}ApoE^{-/-}* and *ApoE^{-/-}* mice, were incubated in RPMI 1640 supplemented with 10% (v/v) heat-inactivated foetal calf serum (HIFCS), 50 IU/ml penicillin G, 50 μ g/ml streptomycin, 2 mM glutamine with 10 mM HEPES, and 20% (v/v) L-cell conditioned medium as a source of M-CSF (Du et al., 2015). Macrophages were considered fully differentiated after 7 days; viability was determined by Trypan blue exclusion. *Phagocytosis assay* – Macrophages in RPMI 1640 supplemented with 50 IU/ml penicillin G, 50 μ g/ml streptomycin, 2 mM glutamine with 10 mM HEPES, were serum-starved overnight. Phagocytosis was assessed the following day using the Phagocytosis Assay Kit (Cayman Chemical) according to manufacturer's instructions. Analysis was performed using a BD FACSVerser flow cytometer as above.

Cholesterol loading and efflux – For cholesterol loading studies, macrophages at 5×10^5 per well in a 12 wtp were incubated in complete medium containing 25 μ M acLDL for 48 h, followed by 2X PBS washes and 16 h equilibration in RPMI containing 1% FBS. Cells were washed 2X in PBS prior to harvest or efflux. For efflux studies, acLDL was incubated with 3 H-cholesterol overnight at 4°C and then added to complete medium at 2 μ Ci/25 μ g acLDL, and cells treated as above. Efflux was induced by incubating cells in RPMI containing 0.1% BSA (fatty acid free; Sigma Aldrich) ApoA1(5 μ g/ml)

for 4 h. ^3H was counted by liquid scintillation for radioactivity in media and cells, and efflux calculated as (counts in media/counts in media and cells) (Du et al., 2015).

Flow cytometry – Bone marrow harvested from femurs and tibiae underwent brief red blood cell lysis, resuspended in HBSS and incubated with a cocktail of antibodies that react with lineage-committed cells and stem cell markers as described by us (Murphy et al., 2011). Analysis was performed on a BD FACS CantoII flow cytometer. Macrophages were harvested and counted, blocked in PBS containing 5% heat inactivated normal rabbit serum, 0.5% BSA, 2 mM NaN_3 and mouse FcR blocking reagent (Miltenyi Biotec Australia Pty. Ltd.), washed in PBS containing 1% HIFCS and 2 mM NaN_3 and incubated with antibodies to CD11b-BV510 and F4/80-BV421 (BD Biosciences). Flow cytometry was performed using a BD FACSVerser and analyzed using FCS Express (De Novo Software).

Apoptosis assay - macrophages were differentiated for 7, 14, or 21 days. Cells were stained with Annexin V (Invitrogen) according to manufacturer's instructions and analyzed by flow cytometry within 1 h. Results expressed as annexin V staining as a percentage of the total cell population.

Efferocytosis assay – Macrophages were seeded onto glass coverslips. Apoptotic thymocytes (treated with 5 μM dexamethasone for 12 h; ~95% Annexin V positive) were stained with CFSE (Invitrogen), as per manufacturer's protocol and added 1:10 (macrophage:thymocyte). Co-cultures were incubated for 2 h, and then thoroughly washed to remove non-efferocytosed cells. Cells were fixed in 10% neutral buffered formalin, and macrophages were stained with F4/80-BV421 (BD Biosciences). 3-9 images were taken on a Zeiss Axio Imager Z2 microscope. Efferocytic index was quantified as the number of macrophages that contained thymocytes as a ratio of total macrophages in the image (Khanna et al., 2010).

Migration assay – Macrophages (10^6 in 100 μl) were plated onto 5 μm transwell filters (Costar), incubated for 2 h in RPMI 1640 then filter inserts transferred to wells containing 600 μl recombinant murine CCL-19 (0.1 $\mu\text{g/ml}$; R&D Systems), and incubated at 37°C for 24 h. Cells that had migrated through the filter were counted manually.

Metabolomic Profiling - Deproteinized plasma extracts from 6 w old *Trail*^{-/-} and wildtype, and bone marrow chimera mice were subjected to normal phase hydrophilic interaction chromatography (Kimberly et al., 2017). Metabolite peaks were integrated using Sciex MultiQuant software. All metabolite peaks were manually reviewed for peak quality in a blinded manner. In addition, pooled cellular extract samples were interspersed within each analytical run at standardized intervals every 10 injections, enabling the monitoring and correction for temporal drift in mass spectrometry performance. The nearest neighbor flanking pair of pooled plasma was used to normalize samples in a metabolite-by-metabolite manner. Internal standard peak areas were monitored for quality control and individual samples with peak areas differing from the group mean by >2 standard deviations were reanalyzed.

Transcriptome profiling - Total RNA from aortae of 6 w old *Trail*^{-/-} and C57Bl6/J wildtype mice (n=3) was interrogated using Affymetrix MoGene 1.0 ST v1.0 gene arrays according to Ramaciotti Centre for Genomics (University of New South Wales, Australia). This data has been deposited in Gene Expression Omnibus GEO DataSets:GSE107645. Interrogating probes were normalized using a robust multi-array average (RMA) algorithm and RMA background corrected (Partek Genome Suite, Partek). Quantile normalization and median polish was used for probeset summarization, in log₂ space. Principle Component Analysis was used to identify distinct gene expression between the two groups. One-way ANOVA of *Trail*^{-/-} vs. wildtype, with unadjusted $p < 0.05$, identified differentially expressed genes. Post-hoc analysis i.e. false discovery rate was considered but was too stringent and biologically significant genes were filtered out as described (Ng et al., 2010). Thus, differentially expressed genes (at unadjusted $P < 0.05$) were used for further analysis. Hierarchical clustering of differentially expressed genes was performed by complete linkage using Euclidean distance as a similarity metric to identify co-regulated or functionally-related genes affected by TRAIL deletion. Gene Set Enrichment Analysis according to Gene Ontology (GO) was used to identify specifically enriched regulatory pathways affected by TRAIL deletion.

Western blotting – Cells were lysed in RIPA buffer. Proteins were resolved on Bolt 4-12% Bis-Tris Plus Gels (Invitrogen, Australia) and transferred onto a nitrocellulose membrane (iBlot 2 Transfer Stacks; Invitrogen, Australia). Membranes were blocked with 5% skim milk, followed by incubation

with primary antibodies; β -actin (15 min, 1:30000, Sigma); nuclear factor-kappa B (NF κ B) p65 was detected using a mouse monoclonal antibody (overnight, 1:1000, Abcam) and phosphorylated NF κ B p65 (p-NF κ B p65, overnight, 1:1000, Abcam). Horseradish peroxidase-conjugated secondary antibodies (Dako) were used and signal detected by chemiluminescence (ECLTM, Western blotting detection reagent, GE Healthcare, Chalfont St Giles, Buckinghamshire, UK)

Chromatin immunoprecipitation (ChIP) – performed as previously described (Chan et al., 2010) using human monocytes treated with 30 ng/ml IL-18 overnight. The immunoprecipitation step was performed using 0.5 μ g NF κ B (Abcam) or rabbit IgG (Millipore). The human TRAIL promoter was amplified using primer sequences that amplify the NF κ B site (Chan et al., 2010): 5'-GGAGAGCAAGAAAGAGAAGAGAGA-3' (forward), 5'-GTGAGGAAATGAAAGCGAATG-3' (reverse) using SYBER green with cycling conditions 95 °C for 10 min, followed by 40 cycles at: 95°C 10 sec, 60°C 15 sec and 72°C 20 sec.

Statistics – Unless indicated, all results were expressed as means \pm S.E.M. Statistical comparisons were made using Students *t*-tests, Mann-Whitney *U*-tests or one- or two-way ANOVA, with Bonferroni's post-test where appropriate. Analysis was performed in GraphPad Prism Version 7.0 (GraphPad Software). A value of $p < 0.05$ was considered significant. Where necessary, statistical outliers were excluded using the Grubb's test.

SUPPLEMENTAL REFERENCES

Cartland, S.P., Erlich, J.H., and Kavurma, M.M. (2014). TRAIL deficiency contributes to diabetic nephropathy in fat-fed ApoE^{-/-} mice. *PloS one* 9, e92952.

Cartland, S.P., Harith, H.H., Genner, S.W., Dang, L., Cogger, V.C., Vellozzi, M., Di Bartolo, B.A., Thomas, S.R., Adams, L.A., and Kavurma, M.M. (2017). Non-alcoholic fatty liver disease, vascular inflammation and insulin resistance are exacerbated by TRAIL deletion in mice. *Sci Rep* 7, 1898.

Chan, J., Prado-Lourenco, L., Khachigian, L.M., Bennett, M.R., Di Bartolo, B.A., and Kavurma, M.M. (2010). TRAIL promotes VSMC proliferation and neointima formation in a FGF-2-, Sp1 phosphorylation-, and NFkappaB-dependent manner. *Circulation research* *106*, 1061-1071.

Di Bartolo, B.A., Chan, J., Bennett, M.R., Cartland, S., Bao, S., Tuch, B.E., and Kavurma, M.M. (2011). TNF-related apoptosis-inducing ligand (TRAIL) protects against diabetes and atherosclerosis in Apoe (-/-) mice. *Diabetologia* *54*, 3157-3167.

Du, X.M., Kim, M.J., Hou, L., Le Goff, W., Chapman, M.J., Van Eck, M., Curtiss, L.K., Burnett, J.R., Cartland, S.P., Quinn, C.M., et al. (2015). HDL particle size is a critical determinant of ABCA1-mediated macrophage cellular cholesterol export. *Circulation research* *116*, 1133-1142.

Khanna, S., Biswas, S., Shang, Y., Collard, E., Azad, A., Kauh, C., Bhasker, V., Gordillo, G.M., Sen, C.K., and Roy, S. (2010). Macrophage dysfunction impairs resolution of inflammation in the wounds of diabetic mice. *PloS one* *5*, e9539.

Kimberly, W.T., O'Sullivan, J.F., Nath, A.K., Keyes, M., Shi, X., Larson, M.G., Yang, Q., Long, M.T., Vasan, R., Peterson, R.T., et al. (2017). Metabolite profiling identifies anandamide as a biomarker of nonalcoholic steatohepatitis. *JCI Insight* *2*, e92989.

Martinez, G.J., Robertson, S., Barraclough, J., Xia, Q., Mallat, Z., Bursill, C., Celermajer, D.S., and Patel, S. (2015). Colchicine Acutely Suppresses Local Cardiac Production of Inflammatory Cytokines in Patients With an Acute Coronary Syndrome. *J Am Heart Assoc* *4*, e002128.

Murphy, A.J., Akhtari, M., Tolani, S., Pagler, T., Bijl, N., Kuo, C.L., Wang, M., Sanson, M., Abramowicz, S., Welch, C., et al. (2011). ApoE regulates hematopoietic stem cell proliferation, monocytosis, and monocyte accumulation in atherosclerotic lesions in mice. *J Clin Invest* *121*, 4138-4149.

Ng, S.F., Lin, R.C., Laybutt, D.R., Barres, R., Owens, J.A., and Morris, M.J. (2010). Chronic high-fat diet in fathers programs beta-cell dysfunction in female rat offspring. *Nature* *467*, 963-966.

Ravindran, D., Ridiandries, A., Vanags, L.Z., Henriquez, R., Cartland, S., Tan, J.T., and Bursill, C.A. (2017). Chemokine binding protein 'M3' limits atherosclerosis in apolipoprotein E^{-/-} mice. *PloS one* *12*, e0173224.

Robertson, S., Martinez, G.J., Payet, C.A., Barraclough, J.Y., Celermajer, D.S., Bursill, C., and Patel, S. (2016). Colchicine therapy in acute coronary syndrome patients acts on caspase-1 to suppress NLRP3 inflammasome monocyte activation. *Clin Sci (Lond)* *130*, 1237-1246.

Stoneman, V., Braganza, D., Figg, N., Mercer, J., Lang, R., Goddard, M., and Bennett, M. (2007). Monocyte/macrophage suppression in CD11b diphtheria toxin receptor transgenic mice differentially affects atherogenesis and established plaques. *Circulation research* *100*, 884-893.

Yu, H., Stoneman, V., Clarke, M., Figg, N., Xin, H.B., Kotlikoff, M., Littlewood, T., and Bennett, M. (2011). Bone marrow-derived smooth muscle-like cells are infrequent in advanced primary atherosclerotic plaques but promote atherosclerosis. *Arteriosclerosis, thrombosis, and vascular biology* *31*, 1291-1299.

Zhao, Y., Pennings, M., Hildebrand, R.B., Ye, D., Calpe-Berdiel, L., Out, R., Kjerrulf, M., Hurt-Camejo, E., Groen, A.K., Hoekstra, M., et al. (2010). Enhanced foam cell formation, atherosclerotic lesion development, and inflammation by combined deletion of ABCA1 and SR-BI in Bone marrow-derived cells in LDL receptor knockout mice on western-type diet. *Circulation research* *107*, e20-31.